Nuclear Materials and Energy 1 (2015) 1–7

Contents lists available at ScienceDirect

Nuclear Materials and Energy

journal homepage: www.elsevier.com/locate/nme

Thermally activated reaction–diffusion-controlled chemical bulk reactions of gases and solids

S. Möller *, A. Kreter, Ch. Linsmeier, U. Samm

Forschungszentrum Jülich GmbH, Institut für Energie- und Klimaforschung – Plasmaphysik, 52425 Jülich, Germany

ARTICLE INFO

Article history:
Received 12 September 2014
Accepted 12 November 2014
Available online 5 February 2015

ABSTRACT

The chemical kinetics of the reaction of thin films with reactive gases is investigated. The removal of thin films using thermally activated solid–gas to gas reactions is a method to in-situ control deposition inventory in vacuum and plasma vessels. Significant scatter of experimental deposit removal rates at apparently similar conditions was observed in the past, highlighting the need for understanding the underlying processes. A model based on the presence of reactive gas in the films bulk and chemical kinetics is presented. The model describes the diffusion of reactive gas into the film and its chemical interaction with film constituents in the bulk using a stationary reaction–diffusion equation. This yields the reactive gas concentration and reaction rates. Diffusion and reaction rate limitations are depicted in parameter studies. Comparison with literature data on tokamak co-deposit removal results in good agreement of removal rates as a function of pressure, film thickness and temperature.

1. Introduction

In vacuum, films can be grown by deposition from the vapour phase. All species present in the vapour can, in principle, constitute to the growing film material inventory. The structural and compositional properties of the films strongly depend on the deposition conditions [1], e.g., temperature, gas pressure and species. If the films grow in the presence of supra-thermal particles, e.g. ions from plasmas, the impact energy provides an additional degree of freedom. The contact of the growing film with plasmas in general leads to a variety of chemical and physical interactions [2], influencing growth rates, films structure and composition. In plasma chambers, these interactions also lead to material migration by sputtering and deposition. Non-volatile, sputtered material can form deposits on vacuum vessel surfaces, which can be porous. Especially in magnetic nuclear fusion devices, material in contact with the plasma is intensively sputtered, transported and deposited by interactions with the energetic plasma particles with ion impact energies ranging from some eV to some keV. Upon deposition, these materials can incorporate also plasma species, e.g. hydrogen isotopes from the nuclear fusion plasma [3], forming so-called co-deposits. If tritium is used as fuel for the nuclear fusion reaction, its retention by this co-deposition becomes a safety and self-sufficiency issue [4,3]: as a D-T nuclear reaction consumes the radioactive isotope tritium, it needs to be bred by the emitted neutron. Losses of tritium (and neutrons) need to be minimized in order to be able to produce at least one tritium per burned tritium to obtain self-sufficiency. Co-deposition is expected to be the dominant hydrogen isotope retention mechanism for many materials (e.g. beryllium or carbon) in consideration for future fusion devices [3], where about 10% of the injected hydrogen isotopes can be retained by co-deposition, rendering it necessary to be able to deplete and, if possible, also remove the co-deposits. In addition to the retention, deposit accumulation and delamination (flaking) are negative aspects of the plasma induced deposition. Through the plasma-surface interaction, these surface modifications can couple back to the plasma, altering its properties. To mitigate this negative impact and maintain reproducible device conditions in fusion as well as non-fusion plasma devices, the deposits need to be removed.

Carbon was, so far, a standard material for nuclear fusion experiments due to its advantageous properties for high temperature plasma operation. The related co-deposits are the so-called amorphous hydrogenated carbon (a-C:H) layers. These layers are formed by the interaction of carbon plasma-facing components with the hydrogen based plasmas. They contain significant amounts (up to >50 atom %) of hydrogen isotopes (H, D, T). The existence of several volatile hydrocarbons leads to the accumulation of a-C:H predominantly on surfaces not in direct contact with the plasma (remote areas) [5]. While other materials are chemically less affine to hydrogen than carbon, co-deposits can still contain relevant amounts of hydrogen isotopes, e.g. some 10% in beryllium co-deposits[3] or about 1% in tungsten co-deposits [6].

One of the possible approaches to remove deposits (and recover hydrogen isotopes) in situ is thermo-chemical removal (TCR), also known as baking in reactive gases. This method is based on the

* Corresponding author.
E-mail address: s.moeller@fz-juelich.de (S. Möller).

http://dx.doi.org/10.1016/j.nme.2014.11.002

formation of volatile species by thermally activated, chemical reactions between a reactive gas and the heated co-deposits on the vessel surfaces. The volatile species can be removed from the vessel by pumping and chemically reprocessed to recover the hydrogen isotopes. Due to working pressures in the range of 1 to 100 kPa and arbitrary exhaust gas partial pressures the product pumping rate is usually not limiting the in-situ removal rate of this method. As a method based on neutral gas, all hot surfaces are affected, also remote areas. Numerous experiments were conducted to evaluate the effect of the different experimental parameters (reactive gas pressure, exposure temperature, etc.) on the removal rate of different constituents. It was shown that the temperature relation is well described by the Arrhenius function in a certain range [7,8]. A linear correlation between the initial co-deposit inventory and its removal rate was observed and accounted to bulk reactions [8]. Higher gas pressure was seen to increase the removal rate, saturating at pressures above ~10 kPa for O_2 as the reactive gas on carbon co-deposits [9]. Time-resolved measurements showed a non-linear time evolution of the removal rate during the procedure [10,11]. Several models, e.g. the Arrhenius model for the temperature relation, were developed for the different parameters. A comprehensive and physical description of the involved processes, connecting the observations on pressure, temperature and inventory relations is still lacking. The present work is intended to provide a qualitative and quantitative understanding of the underlying physics and chemical kinetics of TCR.

The gas permeability of the co-deposits is of central importance within the presented model, explaining the observations regarding gas pressure, inventory scaling and the speed of the process itself. The porosity of a-C:H layers formed by plasmas was described e.g. in [12–14]. Typical values of the relative volume porosity in the order of 10% with pore size distributions centred below 1 nm were observed in a-C:H layers. Permeation experiments yielded coefficients in the order of polyethylene terephthalate plastics [15]. The presented model is based on reaction–diffusion processes, which combines gas diffusion through the material and the reactions occurring in the material [16–18]. This model is able to connect and extend the description of the process concerning the relation to the reactive gas pressure, surface temperature, initial material inventory, co-deposit thickness and the time evolution, thus allowing for comparison with experimental data.

2. Reaction–diffusion model

2.1. General description

All inner and outer surfaces of the co-deposits provide adsorption sites for the injected reactive gas. This reservoir is filled by the reactive gas influx to the co-deposit. The density of reactive gas particles in this reservoir defines the density of reaction partners available for material removal. From the outer surface and, if present, inner surface (porosity) adsorption sites, the reactive gas can penetrate into the material. Subsequently to the adsorption, chemical reactions take place in the volume, depending on the penetration and reactive loss processes. If no accessible inner surfaces (open porosity) are available, reactive gas can permeate through the bulk into the volume. The permeation of reactive gas from inner surfaces into the bulk will be neglected in the mathematical treatment since this only scales the maximum loading coefficient q_{Max} (see below), which is not described analytically here. The volatile products, the exhaust gas, leave the material by diffusion and desorption and can be removed from the vacuum vessel by pumping. The steps of the overall process are depicted in Fig. 1.

In steady state, the diffusive influx of reactive gas particles has to be balanced by the reactive loss to exhaust particles. The diffusion can be seen as a source term for reactive particles at a certain depth x in the co-deposit, balanced by a sink given by the reaction rate k_i of reactive gas particles of density n_{R} with the solid's constituents n_{C} (co-deposit density) to exhaust particles:

$$D * \frac{d^2 n_{\mathrm{R}}(x)}{dx^2} = \sum_i k_i * n_{\mathrm{R}}(x) * n_{\mathrm{C}} \tag{1}$$

Here D is the gas diffusion coefficient and x the depth into the material (Fig. 1). The sum over i is taking all possible reaction paths of the constituent with the reactive gas into account, e.g. the formation of CO and CO_2 by reactions between O_2 as the reactive gas and C in a-C:H as the removed material. A second-order chemical reaction is assumed in Eq. (1). In the following, the sum over all reaction pathways k_i will be omitted without restriction of generality. For solving the differential equation, two boundary conditions are required.

$$n_{\mathrm{R}}(0) = L(p_{\mathrm{Gas}}), \tag{2}$$

$$n_{\mathrm{R}}(\infty) = 0, \tag{3}$$

with a function L describing the adsorption of reactive gas on surfaces at the total gas pressure p_{Gas}. This function also takes into account the adsorption site density and loading, given by the chemical interaction, the available surface area (porosity and outer surface) and gas pressure.

Eq. (2) states that at the surface of the material ($x \to 0$), where the particle transport by diffusion is infinitely fast (compared to reaction losses), the solid contains the amount of the reactive gas which would be adsorbed on its surfaces if reactive losses would be zero. The second condition, Eq. (3), is the result of having the only gas source at the surface (assumption of infinite layer extension perpendicular to x on an impermeable substrate), while having losses by reactions throughout the bulk. Therefore, all reactive gas particles are consumed by reactions at infinite depth. The remaining gas capacity is assumed to fill up with exhaust particles, since the corresponding boundary conditions for exhaust gas are inverted to the ones of the reactive gas. For the exhaust

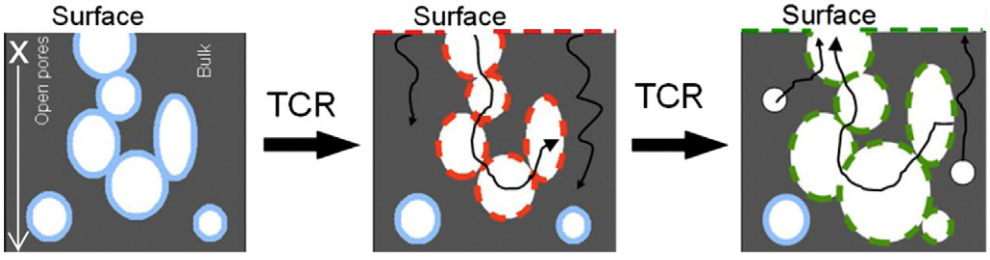

Fig. 1. The three steps of TCR with. Left: An arbitrary mixture of bulk and pores constitute the co-deposit. Centre: The reactive gas diffuses into the pores and adsorbs on all accessible surfaces (red dashed lines). Permeation into the bulk material depends on the material properties. Right: The reactive gas loading interacts chemically with the material (green dashed lines) and forms volatile species. The volatiles leave the co-deposit, material is removed. The reactions can occur in a part or the whole co-deposit volume, depending on the access of reactive gas to the volume. The macroscopic co-deposit density decreases by volume reactions. X indicates the direction used in the mathematical treatment.

gas, sources exist throughout the whole volume, while losses are limited to the surface. With these assumptions the differential Eq. (1) can be solved, yielding

$$n_R(x) = L * e^{-x\sqrt{n_c * k/D}}. \quad (4)$$

With this density distribution of reactive gas particles in the material, the total number n_R of these particles per unit outer surface area can be calculated for a co-deposit of thickness z:

$$N_R(z) = \int_0^z n_R(x)dx = \sqrt{\frac{D}{k * n_c}}\left(1 - e^{-z\sqrt{n_c \frac{k}{D}}}\right) * L \quad (5)$$

Inserting this equation into a second-order chemical reaction equation, describing the reaction between two particles [19], the total number of reactions R_L per unit surface and time is obtained as follows:

$$R_L(T_S,\ p_{Gas},\ z) = k * N_R(z) * n_C = k * \sqrt{n_c \frac{D}{k}} * \left(1 - e^{-z\sqrt{n_c \frac{k}{D}}}\right) * L * n_C\ . \quad (6)$$

The reactive gas adsorption L can be described by the physical models of Langmuir (Eq. (7)) or BET (Brunauer, Emmett, Teller) (Eq. (8)) with the following formulae [20]:

$$L_L(p_{Gas}) = \frac{q_{Max} K_L p_{Gas}}{1 + K_L p_{Gas}}, \quad (7)$$

$$L_{BET}(p_{Gas}) = \frac{q_{Max} * K_{BET} * p_{Gas}}{(p_{Sat} - p_{Gas}) * \left(1 + \frac{(K_{BET} - 1) p_{Gas}}{p_{Sat}}\right)}, \quad (8)$$

where K_L and K_{BET} are the adsorption coefficients in the Langmuir and BET theory, respectively, q_{Max} is the maximum loading of reactive gas particles per volume and p_{Sat} is the pressure at which a monolayer saturation occurs. The Langmuir model is based on single layer adsorption on surfaces and is thus simpler than the BET model, which also describes multilayer adsorption of gas particles occurring at higher pressures. The functions are depicted in Fig. 2 with a set of parameter variations. Significant differences between both adsorption models arise only at higher pressures, as suggested by their physical understanding. Both models show a similar behaviour in the low pressure range, while significant differences can be observed for higher pressures due to multilayer adsorption present only in the BET model. The model coefficients, which are physically based on the interaction potentials of reactive gas and solid and surface (and porosity) properties, determine the amount of adsorbed gas N_R and thus strongly influence the resulting removal rate at a given pressure.

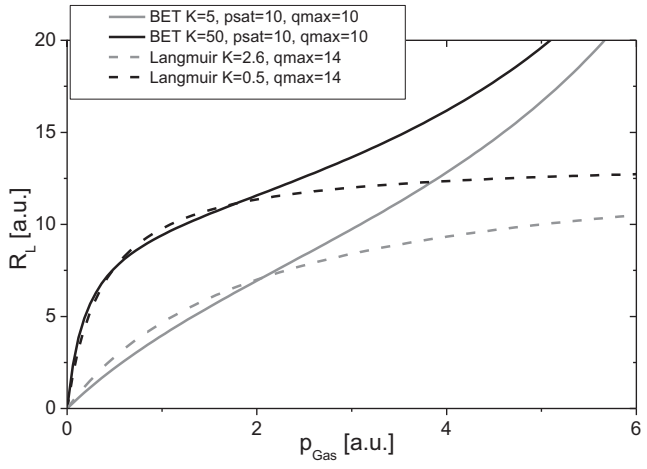

Fig. 2. Comparison of Langmuir and BET theory and the resulting pressure dependence of the removal rate. The value of the adsorption coefficient K influences the amount of adsorbed gas in the material. Note that parameters with similar meaning, e.g. K, do not necessarily have comparable numerical values in both models.

The chemical reaction rate between the material and the reactive gas, coefficient k, can be described by the Arrhenius equation [19], in agreement to numerous observations, e.g. [8,7],

$$k = A * e^{-\frac{E_A}{k_B T_S}}, \quad (9)$$

where A is the collision frequency factor, k_B the Boltzmann constant, E_A the activation barrier energy of the chemical process and T_S the surrounding temperature. This equation describes thermally activated reactions and is thus a physically adequate description. The factor A can be further described by a thermal particle velocity (mass m_R), connected with the collision frequency, and a collision cross-section P:

$$A = P * \sqrt{\frac{\pi k_B T_S}{2 m_R}}. \quad (10)$$

Inserting k from Eq. (9), A from Eq. (10) and L_{BET} from Eq. (8) into Eq. (6), we obtain the following equation for the removal rate of the co-deposit R_L

$$R_L(T_S,\ p_{Gas},\ z) = \sqrt{P * \sqrt{\frac{\pi k_B T_S}{2 m_R}} * e^{-\frac{E_A}{k_B T_S}} * n_c * D} * \left(1 - e^{-z\sqrt{\frac{n_c * P * \sqrt{\frac{\pi k_B T_S}{2 m_R}} * e^{-\frac{E_A}{k_B T_S}}}{D}}}\right) * \left(\frac{q_{Max} * K_{BET} * p_{Gas}}{(p_{Sat} - p_{Gas}) * \left(1 + \frac{(K_{BET} - 1) p_{Gas}}{p_{Sat}}\right)}\right) * n_C\ . \quad (11)$$

For a complete description of the total removal rate R_{Total}, a surface removal term $R_{Surface}$ and an inverse reaction term R_I have to be included in the calculation:

$$R_{Total} = R_L(T_S,\ p_{Gas}, z) + R_{Surface}(T_S,\ p_{Gas}) - R_I \quad (12)$$

In experiments [8,21] with tokamak plasma deposits, about 10 kPa O_2 and about 500 K to 700 K, their contributions were seen to be below the detection limits and thus negligible. For a porous plasma co-deposit, the outer surface area is much smaller than the inner one; thus, $R_{Surface}$ is small compared to R_L. Inverse reactions R_I of the exhaust particles are suppressed due to their endothermic nature.

In nuclear fusion application cases, e.g. the removal of porous a-C:H by O_2 at 623 K, the process is seen to be reaction-limited (see Section 3), i.e., the diffusion D of reactive gas particles into the material occurs much faster than their reactions k with its constituents, as indicated by exposure temperature and co-deposit inventory scalings (e.g.[7,8]).

Whether the removal is in the reaction or diffusion-limited regime is defined by the depth distribution of the reactive gas, which in turn is given by the dimensionless parameter $z\sqrt{n_c k/D}$ (exponent in Eq. (6)). Increasing the material thickness z has a similar effect as a lower diffusion coefficient on the reactive gas density in depth since the diffusion has to pass a longer distance. Thick layers will thus reach diffusion limitation with higher diffusion coefficients D than thin layers. Fig. 3 illustrates the effect of the decisive parameter $z\sqrt{n_c k/D}$ on the reactive gas concentration $n_R(x)$, showing an approximately constant $n_R(x)$ for the reaction-limited case $z\sqrt{n_c k/D} \ll 0.1$. In this case, the reaction rate

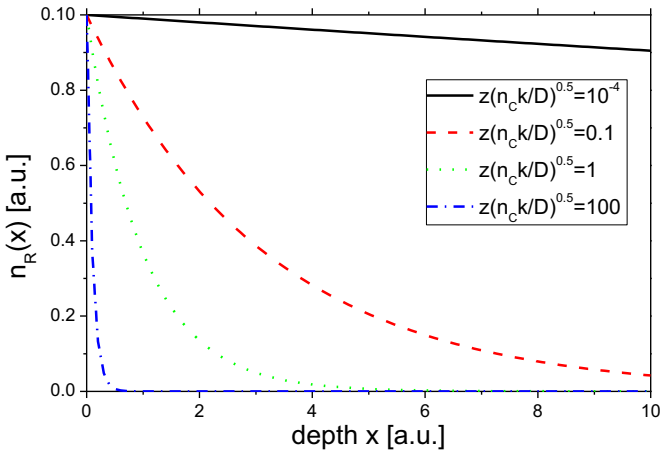

Fig. 3. Parameter study showing the effect of $z\sqrt{n_c k/D}$ on the reactive gas concentration in depth x. The local removal rate is proportional to the local reactive gas concentration (Eq. (6)).

k is small compared to the gas transport relevant parameters z and D, e.g. removal of a thin, porous co-deposit with low exposure temperature and thus k (Eq. (9)). The reactive gas concentration gradient, which drives the diffusive transport, can thus be neglected. The reactive gas concentration is approximately constant in the whole bulk. The higher $z\sqrt{n_c k/D}$ is (e.g. by increasing exposure temperature and thus k), the steeper the concentration gradient becomes. Since the local removal rate in depth x is proportional to $n_R(x)$, the removal will be restricted to a region near the surface and the volume proportionality of the removal rate vanishes for $z\sqrt{n_c k/D} \geq 0.1$. The process with high $z\sqrt{n_c k/D}$ will be called diffusion-limited, and the one with low $z\sqrt{n_c k/D}$ will be called reaction-limited, correspondingly.

2.2. Reaction-limited case

The depletion of reactive gas in depth will lead to a sub-linear scaling with material inventory (given by $z * n_C$). This results in a lower removal rate and a limitation of the reactions to a zone close to the surface. The result of this depletion of reactive gas in depth is shown in the parameter study in Fig. 4. The removal rate first increases with increasing surface temperature (increasing k), according to the Arrhenius function. The slope is reduced below the Arrhenius behaviour at the point where the process changes from reaction to diffusion limitation and the reactive gas starts to get depleted in deeper parts of the layer.

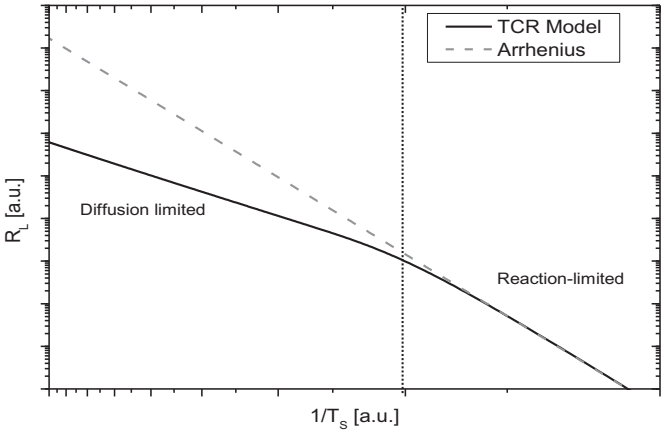

Fig. 4. Arrhenius plot, showing the transition from reaction (low temperature T_S, *right part*) to diffusion (high T_S, *left part*) limitation of thermo-chemical removal (TCR) with temperature (dotted line) and the resulting decrease of the removal rate R_L below the Arrhenius behaviour (dashed line), which is the expectation without reaction partner density effects.

In the reaction-limited case, the exponential depth dependence of n_R is well described by its first-order approximation (see also Fig. 3),

$$e^{-z\sqrt{n_c \frac{k}{D}}} \approx 1 - z\sqrt{n_c \frac{k}{D}}. \tag{13}$$

Under pressures of around 10 kPa of TCR in plasma devices, the Langmuir model for single layer adsorption is sufficient since multilayer adsorption is not relevant. Taking the above into account a simplified relation for the removal rate R_S can be derived from Eq. (6):

$$R_S(T_S, p_{Gas}, z) = P * \sqrt{\frac{\pi k_B T_S}{2 m_R}} * e^{-\frac{E_A}{k_B T_S}} * z * \frac{q_{Max} K_L p_{Gas}}{1 + K_L p_{Gas}} * n_C \ . \tag{14}$$

This approximation of the general Eq. (11) is intended to provide access to the temperature, pressure and thickness relations, while reducing the number of free parameters when fitting to the experimental data. The disadvantage is the non-applicability to diffusion-limited cases.

Formulas describing the parameters K_L and D with certain assumptions can be found in [20,19]:

$$D = r_{Pore} * \sqrt{\frac{\pi k_B T_S}{2 m_R}} \tag{15}$$

$$K_L = K_{L0} * e^{\frac{E_{AS}}{k_B T_S}} \tag{16}$$

with the adsorption binding energy E_{AS}. The calculation of P requires more complex transition state models. With the help of models for those parameters and data for E_A and C_{Por}, ab-initio calculations of the removal rate are possible. However, with the amount of necessary assumptions and the need for additional, error prone measurements (e.g. porosity) a high uncertainty of such calculations is expected. Therefore, the removal rate equations are used without these extensions for the comparison with experimental data. The unknown parameters are obtained by fitting to the experimental data.

Separating the simplified model, Eq. (14), into the relations to z, p_{Gas} and T_S, a set of fitting formulae can be obtained to compare the model with experiments:

$$R(z) = C(T_S, p_{Gas}) * z \tag{17}$$

$$R(p_{Gas}) = C(T_S, z) * \frac{K_L p_{gas}}{1 + K_L p_{gas}} \tag{18}$$

$$R(T_S) = C(z, p_{Gas}) * \sqrt{T_S} * e^{-\frac{E_A}{k_B T_S}} \tag{19}$$

These relations tackle only one parameter, respectively, while the others are condensed into a proportionality factor C, which can be obtained by fitting to experimental data. The influence of co-deposit and reactive gas interaction properties (E_A, D, m_R and P) is also included in the constants.

3. Comparison to literature data on tokamak deuterated carbon co-deposit removal

In this section, the physical understanding presented in the last section, especially the simplified removal rate R_S, is used to interpret experimental results on TCR of deuterated a-C:H deposited in tokamaks. The a-C:H deposits in tokamaks are not well-defined, high-purity material but contain at least several atomic percent of other constituents, e.g.

boron. The simplified model is included in an accompanying study extending the literature data on TCR with NO_2 [21]. The new data presented there are in good agreement with the model presented here and show the higher reaction rate of NO_2 compared to O_2 with a-C:H. The removal times achieved by TCR were about 60 min for 85% D removal by O_2 at 350 °C and 2.1kPa[22], which was reduced to 3 min by NO_2 [21]. The application of other reactive gases, e.g. Fluor or H_2O_2, may further decrease this time by affecting the diffusion and adsorption coefficients and the activation energy E_A, but unintentional effects on other materials also have to be considered. The importance of the co-deposit properties for the TCR rates has to be pointed out. The trends of the removal rate with pressure, temperature and inventory will be similar, but the quantitative removal rates can differ between deposits formed in different (plasma) conditions.

The experiment presented by Davis and Haasz [8] shows the initial deuterium removal rate of TCR in relation to the initial deuterium inventory of the a-C:H deposited in the JET and DIII-D tokamaks. The initial deuterium and carbon inventory can be directly connected to the layer thickness z, if the deposition conditions and thus the co-deposit properties (density) are constant. For the model, the product of thickness and zn_c, the inventory, is relevant and thus used for model comparison. As stated by Davis and Haasz [8], the measured removal rates exhibit a linear relationship with respect to the initial inventory, with the rate obtained on JET and DIII-D co-deposits being similar. The linearity was seen to be valid for initial deuterium inventories spanning over two orders of magnitude. Eq. (17) connects this observation to the reaction-limited regime, where the reactive gas density is constant throughout the material. Layer thicknesses of 2.5 μm to 270 μm were investigated in these experiments. The linear relation between co-deposit inventory and TCR rate is of central importance for the application, as it defines a fundamental difference in removal behaviour of TCR to methods only affecting the co-deposit surface. Fig. 5 presents fits of the model to the data of Davis and Haasz [8]. Eq. (17) yields a good agreement with a slope of $C = 3 \times 10^{-4}$/s and a non-negligible surface removal term of 8×10^{17}D/m^{2}s. The comparison with the exponential relation included in R_L (Eq. (6)) results in a slightly better fit, indicating a change to the diffusion-limited regime at 5×10^{26} D/m^2 ($z \approx 8$ mm), but with a large uncertainty of the extrapolation.

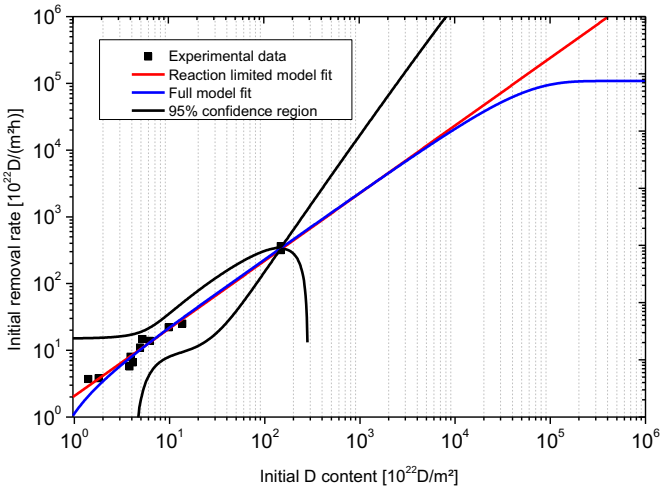

Fig. 5. Fit of the data from Davis and Haasz [8] of 350 °C O_2 TCR on tokamak co-deposits with the simplified, linear model and the full model (with confidence region), including reactive gas depletion effects. In the range of the experimental data points, very good agreement is achieved with both fits, indicating the absence of gas depletion effects (reaction-limited). The full model allows extrapolating to the diffusion-limited regime, but the confidence in this extrapolation is very poor beyond the last data point.

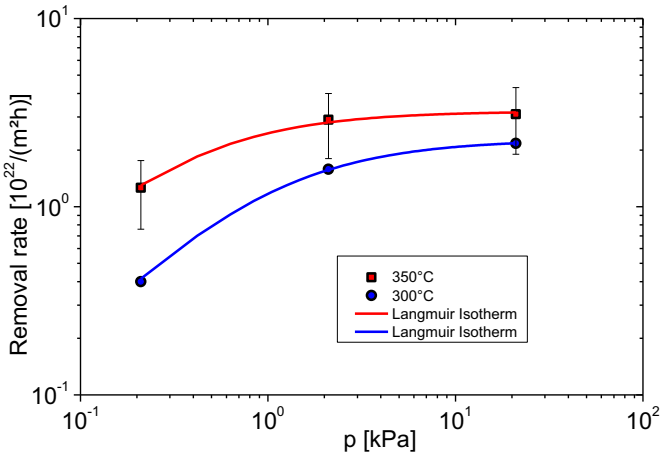

Fig. 6. Fit of the pressure dependence of the removal rate (data from Ochoukov et al. [9]) with a Langmuir adsorption model as predicted by the model (Eq. (18)). A good agreement is found at both temperatures.

Eq. (18) is fitted to data from Ochoukov et al. [9] on the relation between the removal rate and the gas pressure. Fig. 6 shows, that the fit describes the data for both temperatures (300 °C and 350 °C) well, indicating that the Langmuir model is an adequate description of the gas adsorption in TCR. High pressure effects, as described by the BET theory, seem to be negligible in the tested pressure range (0.21–21 kPa).

The relation of the removal rate to the surface temperature was investigated in detail; overviews of a-C:H removal by O_2 are presented in [7,8]. The data exhibit an Arrhenius-like behaviour, which is also a part of the model (Eq. (19)). The scatter can be explained by the use of different material textures [7] and by the normalization to the incident O_2 flux, not taking into account the non-linear pressure effect of gas adsorption on the removal rate (e.g. Eq. (18)). A change of behaviour occurs at temperatures above 1000 K, resulting in removal rates lower than predicted by the Arrhenius relation. In line with these observations by Balden et al. [23], the Arrhenius behaviour for graphite erosion by oxygen was also seen up to 1000 K. The same saturation effect is observed for the deuterium removal rate by O_2-TCR by Davis and Haasz [8], starting at about 700 K. This saturation can be explained by a transition from the reaction to the diffusion-limited regime of the removal process, as shown in Fig. 4. At higher temperatures, the reaction rate k increases according to the Arrhenius relation (Eq. (19)), while the diffusion increases at smaller rates, e.g. Eq. (15). This leads to a depletion of the reactive gas in deeper parts of the material, Fig. 3, as described in the TCR model, Eq. (11). The reduced reaction partner density reduces the local removal rate.

The literature data on O_2-TCR of JET and DIII-D carbon co-deposits presented in this section are used to fit R_S with respect to pressure, temperature and co-deposit inventory. The resulting multi-dimensional fit yields values for all the model parameters, leading to an experimental removal rate function for tokamak plasma a-C:H co-deposits

$$R_{\text{exp-O}_2}(T_S, p_{Gas}, zn_C) = \frac{2.3 \pm 0.2 * 10^{-4}}{s} * \sqrt{\frac{408}{K} T_S} * e^{-\frac{0.35 \pm 0.05 eV}{k_B T_S}} * zn_C * \frac{\frac{2.6 \pm 0.4}{kPa} p_{Gas}}{1 + \frac{2.6 \pm 0.4}{kPa} p_{Gas}} \quad (20)$$

The mass of the O_2 molecule is used for m_R. E_A also includes the thermal activation energy of the adsorption process (K_L) since K_L is chosen temperature independent. $z \cdot n_C$ is giving a value which was also called the inherent content [24] and is here called the inventory.

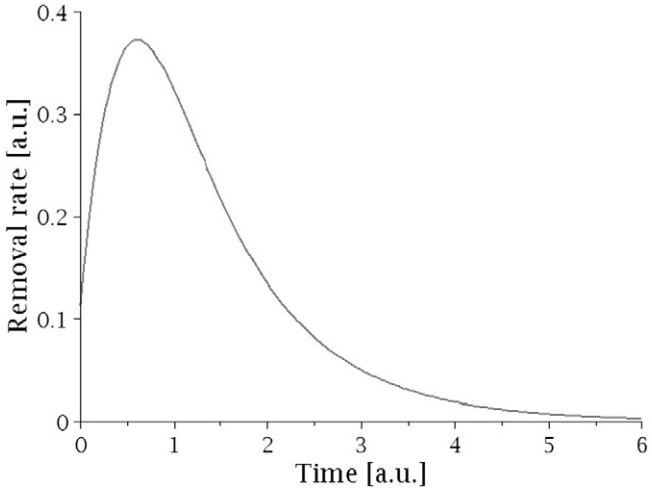

Fig. 7. The time evolution of the TCR rate according to the two competing processes model. Gas capacity increases, while the reaction partner density zn_C decreases, resulting in non-linear behaviour.

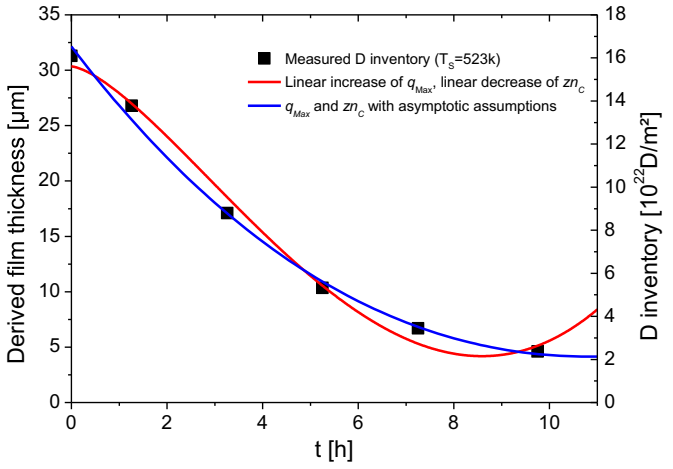

Fig. 8. Time evolution of the D inventory during O_2-TCR fitted with two models for time-dependent q_{Max} and zn_C, data from Haasz and Davis [22]. The asymptotic assumptions on gas inventory and inventory time evolution yield good agreement with the observations. Film thickness was derived by assuming constant layer density, neglecting the effect of bulk removal.

The time evolution of the removal process has also to be addressed, although it is not explicitly included in the presented model. It was seen, e.g. in [10,22,11], that the TCR rate shows a non-linear behaviour with time. An intermediate maximum and smaller rates in the beginning and at the end of the removal process, as sketched in Fig. 7, can be seen in some data [22]. This indicates the presence of two competing processes. Within the scope of the model, the processes can be identified from Eq. (14) as an increase in reactive gas capacity q_{Max} and a decrease of the areal reaction partner density $z \cdot n_C$ with time. The time behaviour of $z \cdot n_C$ and q_{Max} can at this point only be estimated. In principle, all constituents of the material can behave differently in their time evolution since the reactions are different. The time evolution of the removal parameters (e.g. $z \cdot n_C$ and q_{Max}) can even be coupled to only a subset of constituents. For simplicity, an exponential decay is assumed for $z \cdot n_C$. The reaction rate for removing material is proportional to $z \cdot n_C$, leading to a differential equation with an exponential solution for its time evolution. If the material is removed mainly by bulk reactions, it is reasonable to assume that q_{Max} starts at a certain initial value q_{Max0}, determined by the initial material structure and chemical interaction properties. With continuing removal, q_{Max} gradually approaches a maximum, since more surface area is generated by the volume removal. This porosity increase first accelerates the removal, but in the final stage of removal, the porosity growth will decelerate with decreasing bulk and reaction partner density. If this process is not relevant, only the exponential decay in removal rates induced by the $z \cdot n_C$ effect will be observed. In general q_{Max} and n_C can also change depth dependently, if the removal is not perfectly reaction-limited. The time evolution can in conclusion be described by functions asymptotically reaching the maximum $q_{Max\text{-}inf}$ for q_{Max} and zero for $z \cdot n_C$:

$$q_{Max}(x,t) = q_{Max0} + (q_{max\text{-}inf} - q_{Max0}) * \mathrm{erf}(t/\tau_a(R_L)) \quad (21)$$

$$[z * n_C](x,t) = z_0 * n_{C0} * e^{-t/\tau_b(R_L)}, \quad (22)$$

where the initial values are indicated with index *0*. The characteristic times τ_a and τ_b can show a connection to the removal rate R_L, i.e. they will also be related to T_S and p_{Gas}. This model of the time evolution extends the model presented in [17].

The data on TCR time evolution from Haasz and Davis [22] are fitted with the competing process model. As the data were given as total deuterium inventory, the removal rate equation was integrated over time prior to fitting in order to obtain the total amount of removed material. The assumptions of a linear increase of q_{Max} and a linear decrease of the inventory zn_C give a rough agreement (Fig. 8). A better agreement is reached with the Eqs. (21) and (22).

4. Conclusions

An analytical model of the thermo-chemical removal (TCR) process based on reaction–diffusion processes in a permeable material is developed. From the complete description, two limits are derived, the reaction and the diffusion-limited regimes. For the reaction-limited regime a simplified fitting formula, describing the relation between the removal rate (expressed in atoms per area and time) and the material properties, the reactive gas pressure, material temperature and initial inventory is derived. Comparisons of the model with literature data yield good agreement. The good agreement between the new model and the experimental data supports the physical understanding of the importance of the competition of reaction and diffusion processes and the resulting reactive gas density in the material for the removal rates.

The relations shown in the derived equations lead to new approaches for the interpretation of TCR experiments and also for the layout of new experiments and the application. In the framework of the TCR model, material is removed by reactions in the deposit bulk. An important consequence is, as it was already observed by Davis and Haasz [8] for a-C:H layers, that the removal rate by TCR is proportional to the initial inventory zn_C, i.e. the initial deposit thickness z and density n_C, if the removal is reaction-limited. The co-deposit properties and its interaction with the reactive gas (defining reaction rate k, diffusion coefficient D …) are significantly affecting the removal rates by determining the dimensionless parameter $z\sqrt{n_C k/D}$. This parameter is identified to be decisive for determining the penetration of the reactive gas into the deposit and thus the reaction regime. The parameter thus has to be considered when studying the effects of external parameters as the reactive gas pressure or surface temperature.

The material properties, especially the reactive gas capacity (and porosity) and the reaction partner density, can change during the removal process, leading to a non-linear time evolution of the removal rate, which has to be taken into account when comparing different experiments. An approach to explain this behaviour is presented and successfully tested with experimental data from the literature. In agreement with experiments, the removal rate exponentially decreases towards complete removal within this model. This asymptotic behaviour makes a complete deposit removal by TCR impractical in the application. To decrease the operation time loss in application, the

time averaged removal rates can be increased by limiting the removal to a fraction of the initial deposit inventory (e.g. 95%). In this case, a logarithmic scaling of the removal time with inventory is achieved in the reaction-limited regime (small $z\sqrt{n_c k/D}$). The efficiency of the TCR method for hydrogen isotope removal from a-C:H co-deposits in nuclear fusion reactors can be optimised by several means. The new understanding enables to optimise the removal rates systematically by the choice of $z\sqrt{n_c k/D}$ and the consideration of the time evolution.

Although the presented model is developed and tested with a-C:H layers in mind, it is not necessarily limited to them. Moreover, the only assumptions are chemical reactions between the gas and the solid forming volatiles, the loss of these volatiles from the material and the two stated boundary conditions of gas influx at a single outer surface and the possibility of reactions throughout the bulk. Porosity and significant gas inventories were observed not only for carbon [12] but, e.g. also for beryllium co-deposits [25] and can be expected for other co-deposits formed in plasma devices [1]. Thus, TCR and its description by the presented model may be applicable to all deposits. If a layer has constituents that are not forming volatiles with the reactive gas, e.g. W and Be with O_2, these constituents cannot be removed by TCR, as they will not be removed from the deposit. This can influence the removal of other deposit constituents and the time evolution of the process can change. The new understanding of TCR may, for the first time, allow applying the method in a controlled way to nuclear fusion devices, possibly solving the tritium retention issue especially related to carbon based materials.

Acknowledgements

The authors thank Dr. Carolina Björkas for supporting the publication and providing her competence in the field of co-deposits.

References

[1] J.A. Thornton, Annu. Rev. Mater. Sci. 7 (1977) 239.
[2] R. Behrisch, W. Eckstein, Sputtering by particle bombardment: experiments and computer calculations from threshold to MeV energies, Springer, Berlin, 2007.
[3] J. Roth, et al., Plasma Phys. Control. Fusion 50 (2008) 103001.
[4] M.A. Abdou, E.L. Vold, C.Y. Gung, M.Z. Youssef, K. Shin, Fusion Technol. 9 (1986) 250–285.
[5] J. Coad, M. Rubel, N. Bekris, D. Brennan, D. Hole, J. Likonen, E. Vainonen-Ahlgren, Fusion Sci. Technol. 48 (2005) 551–556.
[6] J. Roth, K. Schmid, Phys. Scr. T145 (2011) 014031.
[7] J.W. Davis, A.A. Haasz, Phys. Scr. T91 (2001) 33–35.
[8] J.W. Davis, A.A. Haasz, J. Nucl. Mater. 390–391 (2009) 532–537.
[9] R. Ochoukov, A.A. Haasz, J.W. Davis, Phys. Scr. T124 (2006) 27–31.
[10] J.W. Davis, A.A. Haasz, J. Nucl. Mater. (1999) 478–484.
[11] J. Davis, C.K. Tsui, G.A. Chung, B.W.N. Fitzpatrick, A.A. Haasz, J. Nucl. Mater. 415 (2011) S789–S792.
[12] C. Martin, M. Richou, C. Brosset, W. Sakaily, B. Pegourie, P. Roubin, Stud. Surf. Sci. Catal. 160 (2007) 249–256.
[13] G. Kögel, D. Schödelbauer, W. Triftshäuser, J. Winter, Phys. Rev. Lett. 60 (1988) 1550–1553.
[14] L. Jacobsohn, G. Capote, M. Maia da Costa, D. Franceschini, F. F. Jr., Diam. Relat. Mater. 11 (2002) 1946–1951.
[15] S. Vasquez-Borucki, W. Jacob, C.A. Achete, Diam. Relat. Mater. 9 (2000) 1971–1978.
[16] W.R. Wampler, S.L. Allen, N.H. Brooks, C.P. Chrobak, J.W. Davis, R. Ellis, B.W.N. Fitzpatrick, A.A. Haasz, A.G. McLean, P.C. Stangeby, P.L. Taylor, C.K. Tsui, Phys. Scr. T145 (2011) 014025.
[17] W. Wang, W. Jacob, J. Roth, J. Nucl. Mater. 245 (66–71) (1997) 66–71.
[18] K. Maruyama, W. Jacob, J. Roth, J. Nucl. Mater. 264 (1999) 56–70.
[19] C. Czeslik, H. Semann, R. Winter, Basiswissen physikalische Chemie, Teubner, Stuttgart, 2007.
[20] R.M.A. Roque-Malherbe, Adsorption and diffusion in nanoporous materials, CRC Press, 2007.
[21] S. Möller, D. Alegre, A. Kreter, P. Petersson, H.G. Esser, U. Samm, Phys. Scr. T159 (2014) 014065.
[22] A.A. Haasz, J.W. Davis, J. Nucl. Mater. 256 (1998) 65–68.
[23] M. Balden, W.U. Klages, W. Jacob, J. Roth, J. Nucl. Mater. 341 (2005) 31–44.
[24] C. Tsui, A. Haasz, J. Davis, J. Coad, J. Likonen, Nucl. Fusion 48 (2008) 035008.
[25] G.D. Temmerman, et al., J. Nucl. Mater. 390–391 (2009).